Biofilm 3 (2021) 100040

Contents lists available at ScienceDirect

Biofilm

journal homepage: www.elsevier.com/locate/bioflm

Quantitative determination of rapid biomass formation on pyro-electrified polymer sheets

Emilia Oleandro [a,b,*], Romina Rega [a,**], Martina Mugnano [a], Filomena Nazzaro [c], Pietro Ferraro [a], Simonetta Grilli [a]

[a] Institute of Applied Sciences and Intelligent Systems "E. Caianiello", National Research Council of Italy (CNR-ISASI), Via Campi Flegrei 34, 80078, Pozzuoli (Naples), Italy
[b] Università degli Studi della Campania Luigi Vanvitelli, Viale Abramo Lincoln, 5, 81100, Caserta, Italy
[c] Institute of Food Sciences, National Research Council of Italy (CNR-ISA), Via Roma, 64, 83100, Avellino, Italy

ARTICLE INFO

Keywords:
BET carrier
Pyro-electrified polymer sheets
Bacterial adhesion
Biofilm formation
Crystal violet assay

ABSTRACT

The ability of a bacterial strain to form a biofilm is strictly related to its pathogenicity. Bacterial adherence and early biofilm formation are influenced by chemical, physical and biological factors that determine their pathogenic properties. We recently presented in literature the ability of pyro-electrified polymer sheets to promote rapid biofilm formation, based on what we called biofilm electrostatic test (BET) carriers. Here we performed a step forward by presenting a comprehensive characterization of the BET methodology through a quantitative evaluation of the biomass on the BET-carrier in the very early stages of incubation. Two bacterial suspensions of *Escherichia coli* were added to the surface of the BET-carrier, with one order of magnitude difference in initial optical density. The biofilms were stained at different incubation times, while the crystal violet assay and the live/dead reaction kit were used for evaluating the biomass and the viability, respectively. The BET-carrier systematically promoted a faster biofilm formation even in case of very diluted bacterial concentration. The results suggest that the BET-carrier could be used for evaluating rapidly the ability of bacteria to form biofilms and thus their inclination to pathogenicity, thanks to the challenging acceleration in biofilm formation.

1. Introduction

Bacterial contamination in the form of biofilm is a serious problem in many industrial sectors and has significant consequences for human health [1–3]. Therefore, the evaluation of microbial capability to form biofilms is a critical issue for assessing how different environmental factors may affect their viability [4]. The process of bacterial adhesion leading to the biofilm formation is subjected to physical, chemical and biological phenomena, such as the interaction with specific topographic structures [5,6] or with specific pH and adhesive properties [7]. The biofilm develops in different steps including a first physical interaction that is reversible and, successively, through irreversible processes at molecular and cellular level [8–10]. New techniques for detecting and controlling the bacterial cultures are increasingly studied and tested in different fields of research [11–13]. According to the DLVO (Derjaguin, Landau, Verwey, Overbeek) theory, the interaction between the surface and the bacterial cells depends on the resultant of the van der Waals and Coulomb forces [14–18]. The van der Waals force dominates in the region close to the surface while the Coulomb force dominates away from the surface. In general, a charged particle in an aqueous solution tends to attract the free ions in the liquid and leads to the formation of a double electric layer. The cytoplasmic wall of a bacterial cell owns a net negative charge and the same occurs for a natural surface immersed in an aqueous solution [19]. Therefore, both the cell and the surface form a double electric layer and, hence, a repulsive electrostatic interaction occurs. In these conditions, there is a minimum of secondary surface energy outside the energy barrier. The distance between the surface and the minimum secondary surface energy is usually several nanometres long. Successively, the bacterial cells – using flagella or producing exopolymeric substances (EPS) – can perforate the energy barrier and favour the interaction between the cell and the surface, forming an irreversible biofilm. In particular, the EPS is important for establishing the initial

* Corresponding author. Institute of Applied Sciences and Intelligent Systems "E. Caianiello", National Research Council of Italy (CNR-ISASI), Via Campi Flegrei 34, 80078, Pozzuoli (Naples), Italy.
** Corresponding author.
E-mail addresses: e.oleandro@isasi.cnr.it (E. Oleandro), r.rega@isasi.cnr.it (R. Rega).

https://doi.org/10.1016/j.bioflm.2020.100040
Received 3 September 2020; Received in revised form 3 December 2020; Accepted 7 December 2020
Available online 17 December 2020

attachment to the surface, helping the cell to anchor and to stabilize the colony against the environmental fluctuations [7].

Different methods have been proposed in literature for studying and evaluating the formation of a biofilm. The most popular method is based on microtiter plates, where the biofilm is evaluated by measuring the attached biomass. The main limitation is that parts of the biomass can derive from cells sedimented at the bottom of the wells, thus introducing a non-negligible error. To overcome this limitation, the Calgary biofilm device was developed, based on the use of pegs that fit into the wells of the microtiter plate thus preventing the biofilm formation from the sedimented cells. However, still some drawbacks exist because the recovery of the bacterial cells is made by sonication that is able to retrieve only a part. Moreover, the physiological properties of the detached population may not reflect the physiology of the sessile cells, since different populations may exhibit different adhesion and material detachment [20]. The BioFilm Ring Test (Saint- Beauzire, France) uses specific magnetic microbeads that tend to immobilize through the growing biofilm matrix *in vitro*. In other words, when the biofilm is formed, the microbeads become embedded in the matrix. This technology has some limitations for the application in the clinical setting, because it requires the additional step of treating the cells with the magnetic beads, introducing a further variable that could affect the biofilm formation and its repeatability [20,21].

Other studies regard the interaction between bacteria and electrically charged surfaces. Gottenbos et al. [22] observed the behaviour of different Gram-negative bacteria against surfaces with a net positive charge. They reported an enhanced bacterial growth in case of *Pseudomonas aeruginosa* (*P. aeruginosa)*, while they did not observe the formation of a mature biofilm in the case of *Escherichia coli (E. coli)*. Similar studies were made by Harkes et al. [23] who reported similar results, probably due to a disturbance of the positive charge of the surface, which can affect the electrolyte balance on the bacterial membrane. The above-mentioned techniques make use of positive surface charges induced through a chemical functionalization process.

Recently, we presented a simple and voltage-free methodology called pyro-electrification (PE) for inducing a positive permanent charge in polymeric freestanding sheets, through the pyroelectric effect in lithium niobate (LN) crystals. These sheets can promote the adhesion of both eukaryotic and prokaryotic cells [24–28] onto otherwise cytophobic surfaces. Such approach is innovative as it is based on a physical phenomenon that avoids chemical treatments of the surfaces. In particular, we introduced for the first time the Biofilm Electrostatic Test carrier (BET-carrier), demonstrating how the PE sheets enable a biofilm formation 6-fold higher than in case of the control sheet, thus providing a repeatable tool for rapid evaluation of biofilm formation *in vitro* [24], which is an important indicator of the bacterial pathogenicity.

Here a further characterization is presented for this innovative methodology. Considering the peculiar rapidity of biofilm growth on the BET-carrier [24,28], we focused our attention on the first stages of biofilm formation by performing an accurate quantitative evaluation of the biofilm mass by a crystal violet (CV) assay. The biofilm mass adhering on the BET-carrier in the first hours of incubation was determined through optical density (OD) measurements and the viability of the adhering bacteria was evaluated by standard staining procedures. We performed comparative experiments *in vitro* by using two different concentrations of the bacterial suspension, that differ each other by about one of order of magnitude in OD. For brevity we call them "*high OD*" and "*low OD*". Since the technique is new and innovative, we focused our attention on the *E. coli*, a bacterial strain whose pathogenicity is linked to the formation of biofilms [7,29,30].

The results show clearly that, compared to the control surface, the BET-carrier promotes a biofilm with higher maturity in the very early stages of incubation under both *high* and *low* OD. Thus, it allows us to evaluate *in vitro* the ability of bacteria to form biofilms also in case of highly diluted samples. We believe that the reliability of the technique can open a new route in the use of BET for the rapid evaluation of biofilm formation, and therefore of their inclination to pathogenicity.

2. Material and Methods

2.1. Polymer solution

Solid-state polysulfone (PSU) (Mw ~ 35000, transparent pellets) was bought from Sigma Aldrich (Milan, Italy). The PSU is a thermoplastic polymer with a glass transition temperature (Tg) at 180 °C. It was dissolved in anisole (99%, Sigma Aldrich, Milan, Italy) at 60% w/w and then stirred at 70 °C for 6 h. The resulting polymer solution of PSU was stored at 4 °C.

2.2. Bare sheets

The freestanding PSU sheets were obtained by spin coating a glass coverslip (2 × 2) cm^2 sized with the PSU solution at 4000 rpm for 2 min, and then by peeling off accurately just after solvent evaporation. The PSU sheets not subjected to PE were used as control.

2.3. Lithium niobate crystals

The LN crystals were purchased from Crystal Technology Inc. Palo Alto, California, and were in the form of wafers with 500 μm thickness and 3-inch diameter. They were congruent within 0.02 mol % Li_2O, both sides polished and in mono-domain ferroelectric state. The structure of LN at room temperature belongs to the 3 m group and consists of planar sheets of oxygen atoms in a distorted hexagonal close-packed configuration. LN is characterized by a spontaneous polarization (Ps), which changes according to $\Delta Pi\ \alpha\ pi\Delta T$, where Pi is the coefficient of the polarization vector, pi is the pyroelectric coefficient and ΔT is the temperature variation ($pi = -8.3 \times 10^{-5}$ C m^{-2} $°C^{-1}$ for LN at 25 °C). At equilibrium conditions, without any thermal stimulation, the Ps is fully screened by the external screening charge and no electric field exists. In presence of a temperature variation, a charge density surface $\alpha = pi\ \Delta T$, caused by uncompensated charges, appears locally and a high electric field (ENL ~ 10^7 V/m) is generated on the surface of the crystal.

The wafers were cut into (20 × 20) mm^2 sized samples by a commercial precision diamond saw to achieve PE sheets with approximately the same lateral size. Before each use, the crystal samples were rinsed three times in acetone and dried with a nitrogen jet to remove dust and impurities from the surface.

The BET-carriers were obtained by following an appropriate PE process that exploits the electric field generated by the LN crystal through the pyroelectric effect [31–34]. Here we used the electric field generated pyroelectrically to induce permanent net charges on the surface of the polymer sheet. More details on the PE process can be found in the SI.

2.4. Bacterial samples

The experiments were realized on the Gram-negative *E. coli* strain DH5α. The *E. coli* strain was handled following the protocol provided by the supplier [35]. According to this protocol, the optimal conditions for growth correspond to incubation at 37 °C in Luria Bertani (LB) broth (10 g SELECT Peptone 140, 5 g SELECT Yeast Extract, and 5 g NaCl, Thermo Fisher Scientific, Monza, Italy). One day before the experiment, 1 mL of the bacterial suspension was collected and cultured in 9 mL of LB broth medium and placed in a shaker incubator (222DS Labnet International, Inc., Edison, NJ, USA) at 37 °C and 100 rpm for about 14/16 h, to achieve saturation conditions. The growth was stopped, and the bacteria were harvested by centrifugation at 7000 rpm (Centrifuge 5415 R, Eppendorf, Milan, Italy) for 10 min to separate the cells from the medium.

After that, we removed the supernatant and we re-suspended the pellet in LB fresh medium in a volume ratio 1:3 to obtain the final suspension. The OD was measured by the spectrophotometer at 600 nm. Starting from this final suspension two bacterial samples were prepared,

by dilution in LB fresh medium with ratios 1:5 and 1:15, up to a volume of 500 μL in both cases. We measured their OD by the spectrophotometer at 600 nm and we obtained OD = 0.4 and OD = 0.03, respectively, indicated here as *high OD* and *low OD*, for brevity.

2.5. Bacterial growth

The bacterial growth curve was evaluated under standard culture conditions [35]. The day before the experiment, the bacteria were cultured in 9 mL fresh medium (LB) and placed in a shaker incubator (222DS Labnet International, Inc., Edison, NJ, USA). When reached the saturation conditions, an aliquot of bacteria (3 mL) was collected and restored in 27 mL of fresh LB medium.

We placed this bacterial suspension in an incubator at 37 °C and 80 rpm. In order to evaluate the trend of the bacterial growth, an aliquot of this bacterial suspension was taken every half an hour and the corresponding OD was measured by a spectrophotometer at 600 nm. Fig. 1 shows the bacterial growth evolution in about 15 h.

Usually, the growth behaviour is influenced by both the environmental conditions and the genetic properties of the bacteria. This curve presents the traditional exponential phase, in which the bacteria first grow quickly, in this case up to about 7 h, and then reach a stationary phase, where the cell growth equals the cell death. This produces finally a stable number of bacterial cells [36–38]. Since we are interested here at the very early stage of the bacterial growth, the observation was performed up to the stationary phase.

2.6. Crystal violet assay

We stained the biofilm adhering on the control and BET-carrier sheets by using a commercial CV provided by Sigma Aldrich (Milan, Italy). The assay was performed as described by Christensen et al. (1985) [39] making some changes. After bacterial incubation and biofilm formation the content of the dish was aspirated at each observation time and the sheet was washed with 2 mL of sterile phosphate buffer saline (PBS), in order to remove all non-adherent bacteria.

Bacteria adhering on the sheet were fixed by immersion in 500 μL of 99% methanol and left drying for 30 min. Then we moved the sheets into clean dishes and stained the fixed bacteria with 500 μL of CV at 2% of distilled water at room temperature for 10 min. The excess stain was rinsed off by placing the sheet under running tap water. After air-drying the dye bound to the adherent bacteria was re-solubilized with 1 mL of acetic acid at 33% (v/v). The OD of the resulting solution was measured at 600 nm by a standard spectrophotometer (BioPhotometer 6131, Eppendorf, Milan, Italy), in order to quantify accurately the biomass adhered on the sheet. In order to evaluate the zero control, we measured the amount of CV absorbed by the polymer sheets without bacteria, both bare and charged. Three replicates of the experiment were carried out and the OD values were measured by the spectrophotometer at 600 nm. The resulting OD was in average equal to 0.1 and hence negligible compared to the OD values measured in presence of bacteria.

2.7. Viability test

For each observation time two sheets were cultured at the same conditions. One was treated with the CV for quantifying the biomass adhering on the sheet (as already described in the previous section), while the other was treated with a live/dead assay kit (live/dead BacLight Bacterial Viability Kit, Thermo Fisher Scientific, Monza, Italy) [40] in order to evaluate the viability of the adhered biomass. Each sheet was immersed in 2 mL PBS containing Syto 9 and propidium iodide at concentration of 10 μM and 2 μg/mL, respectively, and incubated for 15 min in the dark. The cells with a compromised membrane, which are considered to be dead or dying, were stained red whereas cells with an intact membrane were stained green. We recorded the fluorescence microscope images of the adhered biomass by a standard inverted optical microscope (Axio Vert, Zeiss, Jena, Germany).

2.8. Statistical analysis

The number of replicates for each experiment was adjusted according to the variance obtained. The data in the graphs are all presented as means ± the standard deviation. The t-Student test was performed on all data, and the value obtained was $p < 0.05$, which guaranteed the reliability of the results.

3. Results and discussion

A group of 4 Petri dishes were prepared for evaluating the biomass adhering on the BET-carrier at the early stages of biofilm formation, each containing one PSU sheet: (1): bare sheet as control for the CV treatment; (2) bare sheet as control for the live/dead treatment; (3) BET-carrier with face (+) up for the CV treatment; (4) BET-carrier with face (+) up for the live/dead treatment. Each dish was incubated with the bacterial sample

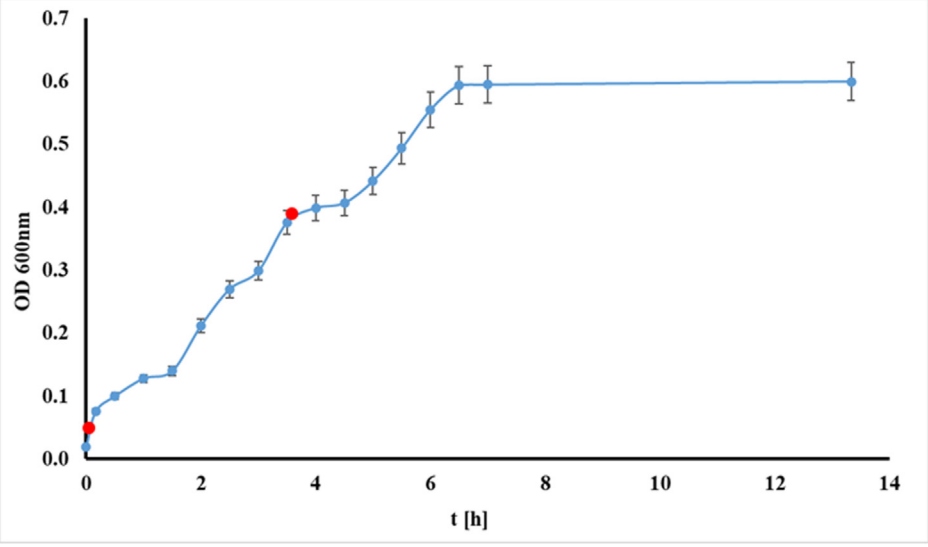

Fig. 1. Growth curve of the *E. coli* strain under standard culture conditions. The two red dots correspond to the low and high OD values used for the comparative experiments. The error bars represent the standard deviation for three replicates of the experiment.

with *high OD* (see Materials and Methods for details) into a volume of 1.5 mL of PBS at 37 °C and 800 rpm. We replicated three times this group of four sheets for evaluating the biomass at three different incubation times: 2 h; 4 h; 6 h.

A comparative study was performed by seeding the same kinds of four sheets with the bacterial sample with *low OD* and, again, three replicates were performed for each of the three incubation times. Therefore, $4 \times 3 = 12$ samples were analysed for each of the two initial OD cases, with a total of 24 samples. Three replicates of the experiments were completed and the results were statistically averaged (see Materials and Methods for details). We cultured the samples in PBS in order to compare the adhesion of planktonic bacteria on the BET-carrier with that on the control sheet, under minimal proliferation effects. The following sections illustrate the results obtained for the two cases of *high OD* and *low OD*.

3.1. The case of high OD

After plating the 12 sheets as mentioned previously, we observed the bacterial adhesion under a standard inverted optical microscope at the three different incubation times (2 h, 4 h, 6 h). Fig. 2 shows the corresponding typical images.

These images show the immobilized bacteria forming biofilm on the control and on the BET-carrier, at different incubation times. The bacteria were dispersed uniformly on both types of surfaces but the number of bacteria on the BET-carrier resulted always higher when compared to that on the control sheet, for all time-intervals observed. This demonstrates how the positive polarization charge on the BET-carrier accelerates the bacterial adhesion respect to the control surface, thanks to a non-negligible electrostatic interaction [11]. According to the DLVO theory [15], the bacteria adhere on the surface when they can overcome the minimal secondary energy.

This process is faster on the BET-carrier compared to that occurring on the bare sheet (control), because the positive polarization charge on the BET-carrier increases the Coulomb interaction strength.

The biomass adhering on the BET-carrier was quantified by the CV assay, analogously to the microtiter-plate test that is most frequently used for the evaluation of biofilm formation [39,41,42].

Fig. 3 shows the typical optical microscope images of the sheets just

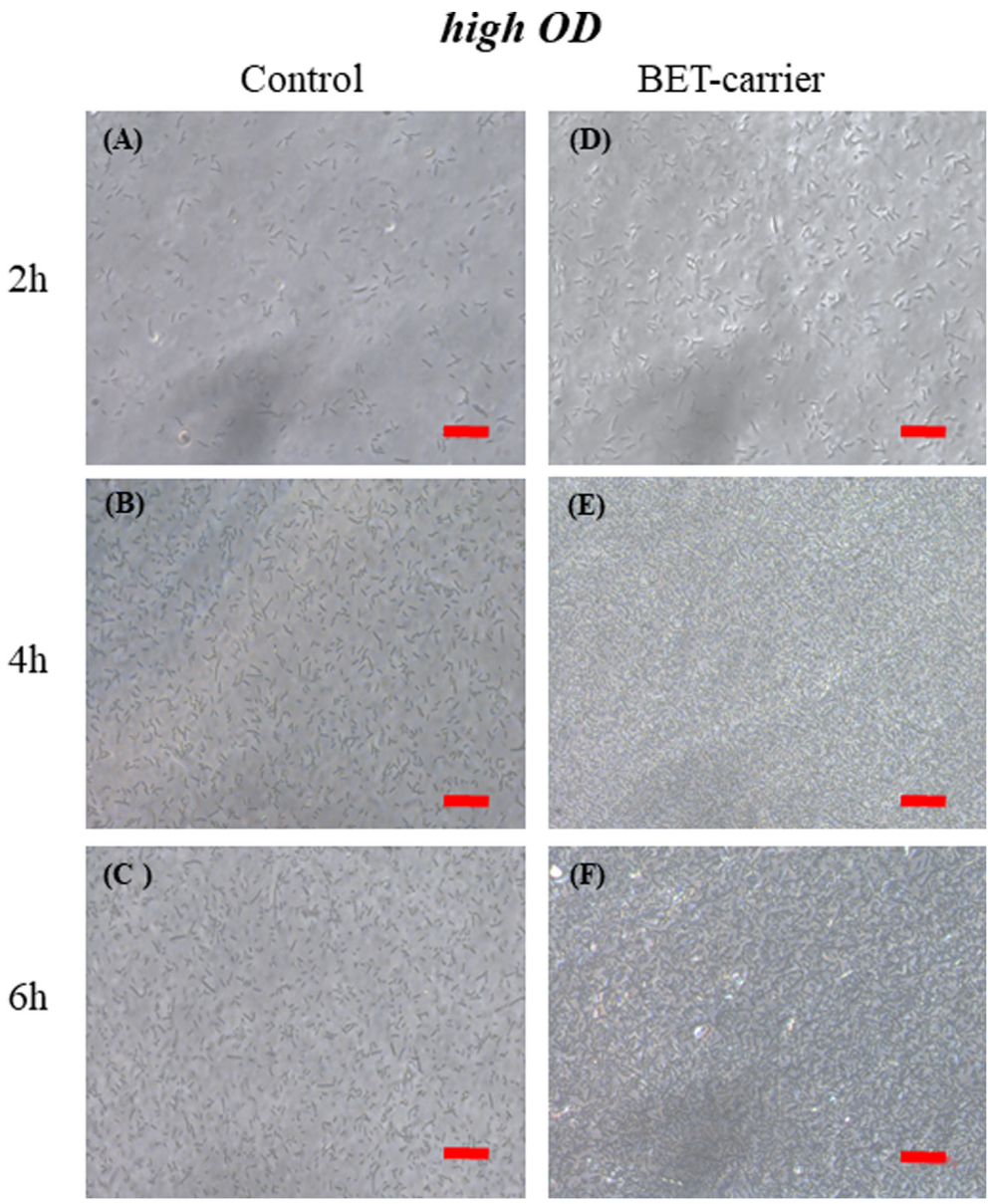

Fig. 2. Case of high OD. Typical optical microscopy images of *E. coli* bacteria forming biofilm on the control sheet (left column) and on the BET-carrier (right column), at three different incubation times. Scale bars indicate 20 μm.

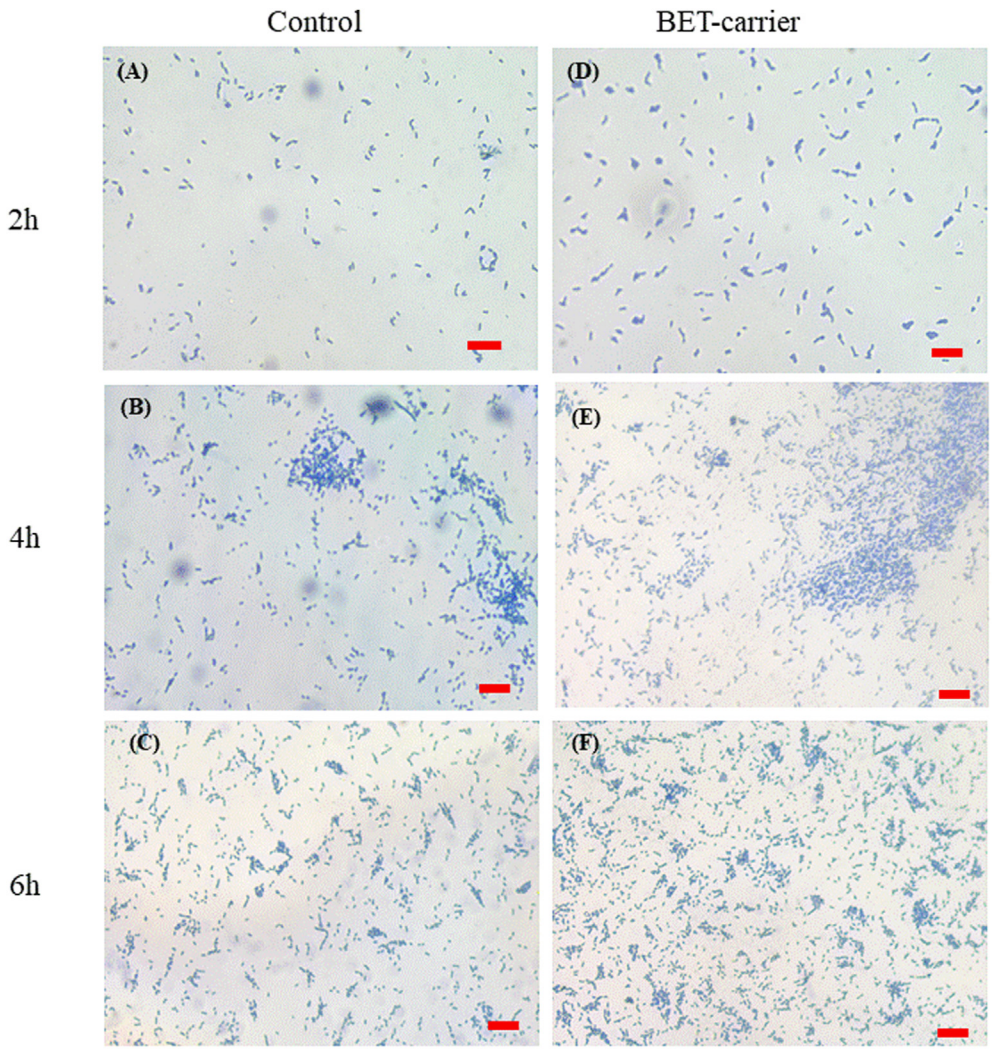

Fig. 3. Case of high OD. Optical microscope images of the *E. coli* bacteria on the control sheets (left column) and on the BET carrier (right column) after CV staining at the three incubation times; Scale bars indicate 20 μm.

after CV staining. Fig. 4 shows the quantification of the biofilm adhered onto the sheets by the absorbance of the CV at 600 nm (OD_{600}) for the control (blue columns) and for the BET-carrier (orange columns), at the three incubation times (2 h; 4 h; 6 h).

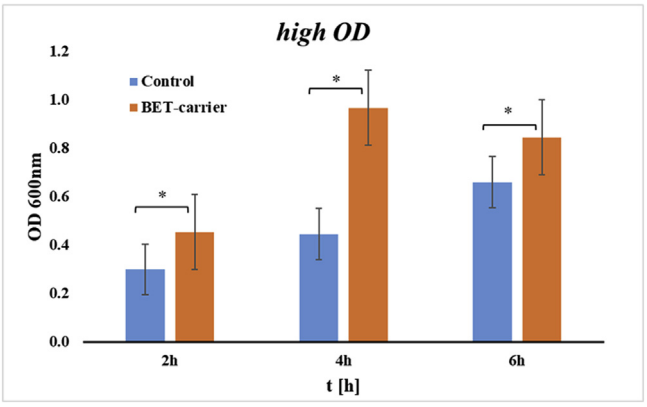

Fig. 4. Case of high OD. Quantitative determination of the biofilm adhered on the sheets by the CV absorbance in case of the control (blue columns) and BET-carrier (orange columns) at the three incubation times. The error bars represent the standard deviation for three replicates of the experiment. Comparison BET-carrier v.s. control considering the different time, * value is $p < 0.05$ has been obtained, which guarantees the reliability of the results.

These data show how the BET-carrier (orange columns) was able to immobilize a higher amount of biomass at each observation time respect to the control, with an increment of about 30% at 2 h and 6 h. It is noteworthy that a much higher increment in biomass was always observed in the case of 4 h incubation, where we had about 60% value of increment in biomass. Moreover, in case of the BET-carrier, at 4 h the biomass was about two-fold higher than that at 2 h. The bacterial biomass on the control sheet at 6 h was even lower than that on the BET-carrier at 4 h. The results in Fig. 4 show that the biofilm mass grew continuously on the control sheet up to 6 h incubation.

Conversely, the biomass on the BET-carrier was, first of all, always higher than that on the control and, moreover, it reached the state of a biofilm with high biomass just after 4 h incubation. This stage on the BET-carrier corresponded to a biofilm with a strong grip on the base and a weaker layer on the top. This was achieved thanks to the strong electrostatic attraction provided by the surface of the BET-carrier, as mentioned before. During the successive 2 h of incubation, the bacterial cells on the top moved away starting a new process of colonization in other sites of the sheet [43, 44]. Therefore, the washing steps performed during the CV assay at 6 h incubation removed the bacterial cells weakly adhered to the top of the biofilm structure, and the detached cells colonized other sites. In case of the control sheet, instead, the biofilm was not

significant within 4 h incubation and therefore new planktonic bacteria continued to adhere to form the 3D structure mentioned above. This agrees with the DVLO theory that describes the biofilm formation in case of charge-free surfaces and confirms that the presence of a surface electric charge accelerates the bacterial adhesion process. Furthermore, the enzymes involved in the exopolysaccharide degradation, in addition to the digestive function, allowed the detachment of the bacteria from the biofilm and hence the colonization of new sites [43,44].

These results demonstrate that 4 h incubation on the BET-carrier can give very rapid information on the ability of bacteria to form biofilm. This could be a tool of great interest in all of those applications that require time-consuming procedures. In particular where it is necessary to test the inclination to pathogenicity, for example in the food industry, where the aim is the extension of the shelf life, or in the clinician field where a rapid antibiogram can save lives [45].

3.2. The case of low OD

The biomass on the BET-carrier was quantified in case of initial OD = 0.03, a value close to the latency phase, in order to evaluate the biofilm formation under highly diluted bacterial suspensions. We performed the same procedures as in case of the *high OD* and we elaborated the results from three replicates of the experiments for both the control and the BET-carrier. Fig. 5 shows the optical microscope images recorded at the three incubation times for the control and the BET-carrier.

It is clear that the number of bacteria adhering on the BET-carrier was always greater than that on the control, at each observation time. The same CV staining procedure was performed as in case of *high* OD, in order to determine the biomass adhering on the BET-carrier in case of a bacterial suspension highly diluted. Three replicates of the experiments were performed and the results averaged.

Fig. 6 (A-F) show the typical optical microscope images of the sheets, just after CV staining. Fig. 7 shows the data corresponding to the biomass determination. In this case the BET-carrier (orange columns) was able to immobilize a higher amount of biomass at each observation time respect to the control (blue columns), with an increment of about 30% and 40% at 2 h and 4 h, respectively. Also in this case, the higher amount of biomass on the BET-carrier was observed at 4 h incubation. It is important to note that the polymer sheets do not exhibit any topography on the surface before the PE process (control) as well as after that (BET carrier). Therefore, the biofilm formation is influenced only by the electrostatic interaction.

These results demonstrate that the BET-carrier is able to produce a biofilm with high biomass within few hours even under very low bacterial concentrations, with a significant impact in all of those applications where the biofilm formation has to be tested starting from highly diluted

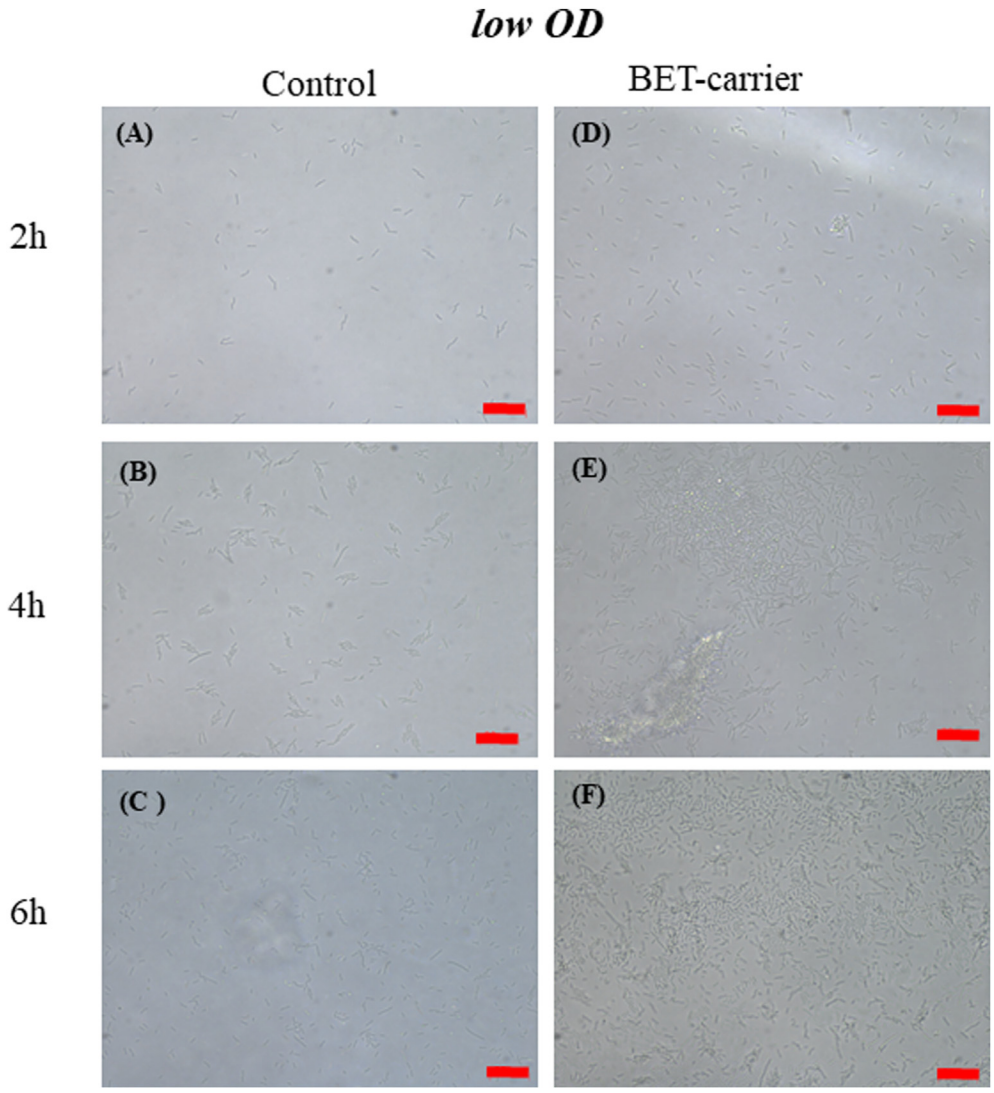

Fig. 5. The case of low OD. Optical microscope images of *E. coli* forming biofilm (A–C) on the control sheet and (D–F) on the BET-carrier at the three incubation times. Scale bars indicate 20 μm.

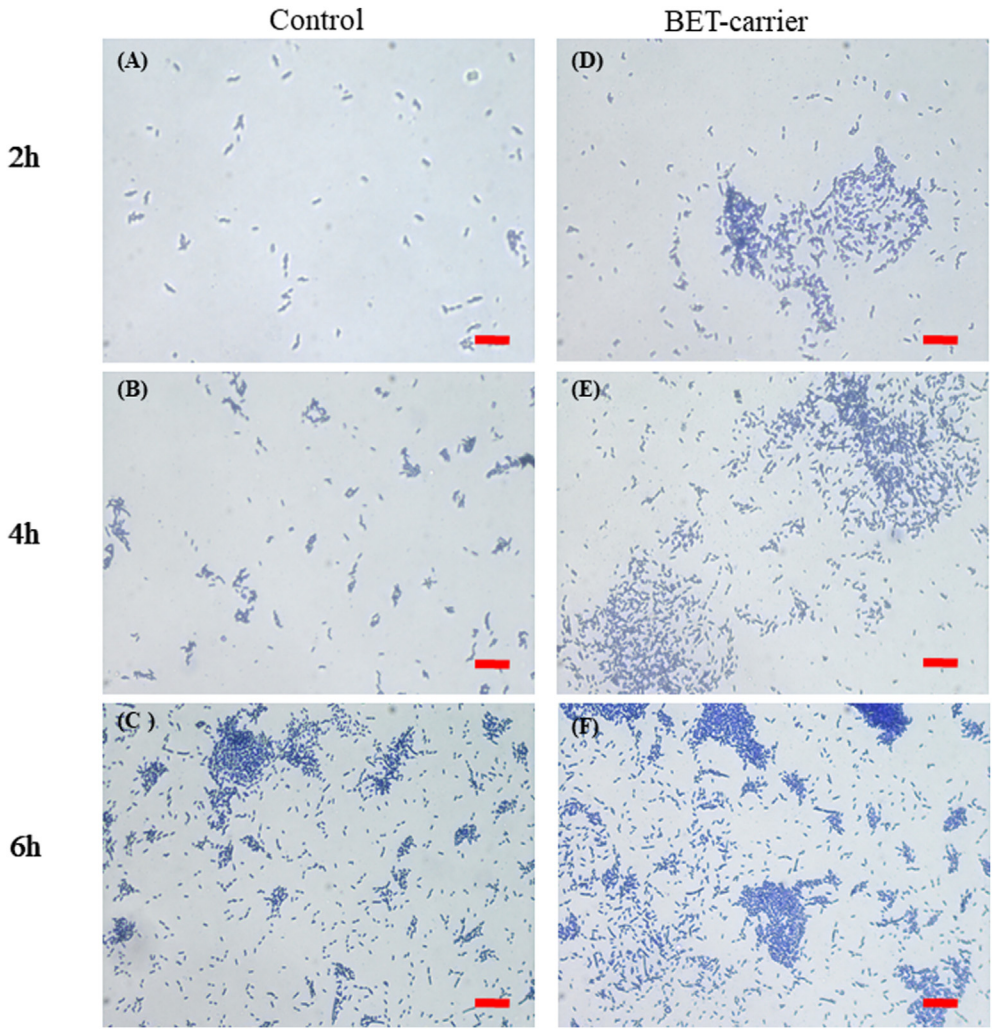

Fig. 6. Case of low OD. Optical microscope images of the control sheets (A–C) and of the BET carrier (D–F) after CV staining at the three incubation times; Scale bars indicate 20 μm.

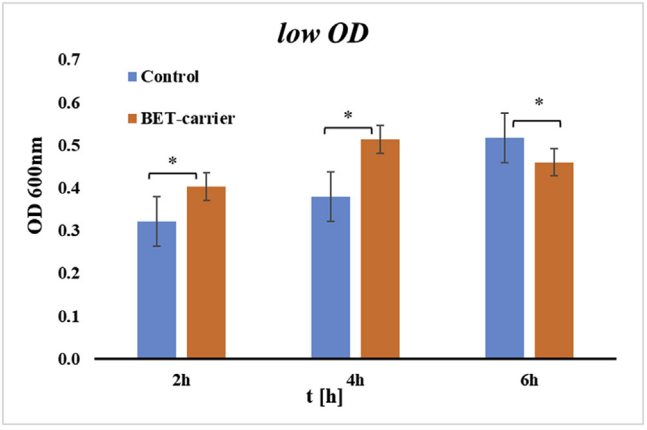

Fig. 7. Case of low OD. Quantitative determination of the biofilm adhered on the sheets by the CV absorbance in case of the control (blue columns) and BET-carrier (orange columns) at the three incubation times. The error bars represent the standard deviation for three replicates of the experiment. Comparison BET-carrier v.s. control considering the different time, * value is $p < 0.05$ has been obtained, which guarantees the reliability of the results.

samples.

3.3. Biomass viability

The biofilm formation is a complex phenomenon that depends on several factors [46]. Here, a faster biofilm formation was achieved by intervening on the physical parameter well described in reference [24]. The PE process induced a permanent dipole in the BET-carrier that, as a consequence, exposed a surface charge δ^+. The bacteria tended to be attracted and immobilized by the surface of the BET-carrier through the interaction with the COO^- groups in their cytomembrane, thus favouring the rapid formation of the biofilm without destroying the cell structure. The viability of the biofilm on the BET-carrier is of fundamental importance for allowing these sheets to be used for efficient antibacterial tests in future. Therefore, we report here the results concerning the viability tests performed on both the control and the BET-carrier, for the three incubation times. A conventional inverted optical microscope (Axio Vert, Zeiss, Jena, Germany) was used for observing the samples after live/dead staining (see Material and Methods for details) and Fig. 8 shows the corresponding results.

Three replicates of the experiments were carried out for the *E. coli* strain, and 10 pictures were captured all around each surface to demonstrate the reliability of the biofilm vitality. The green regions in Fig. 8 (E-F) corresponded to the viable bacteria, whereas the red ones referred to the dead bacteria. These images were analysed by ImageJ

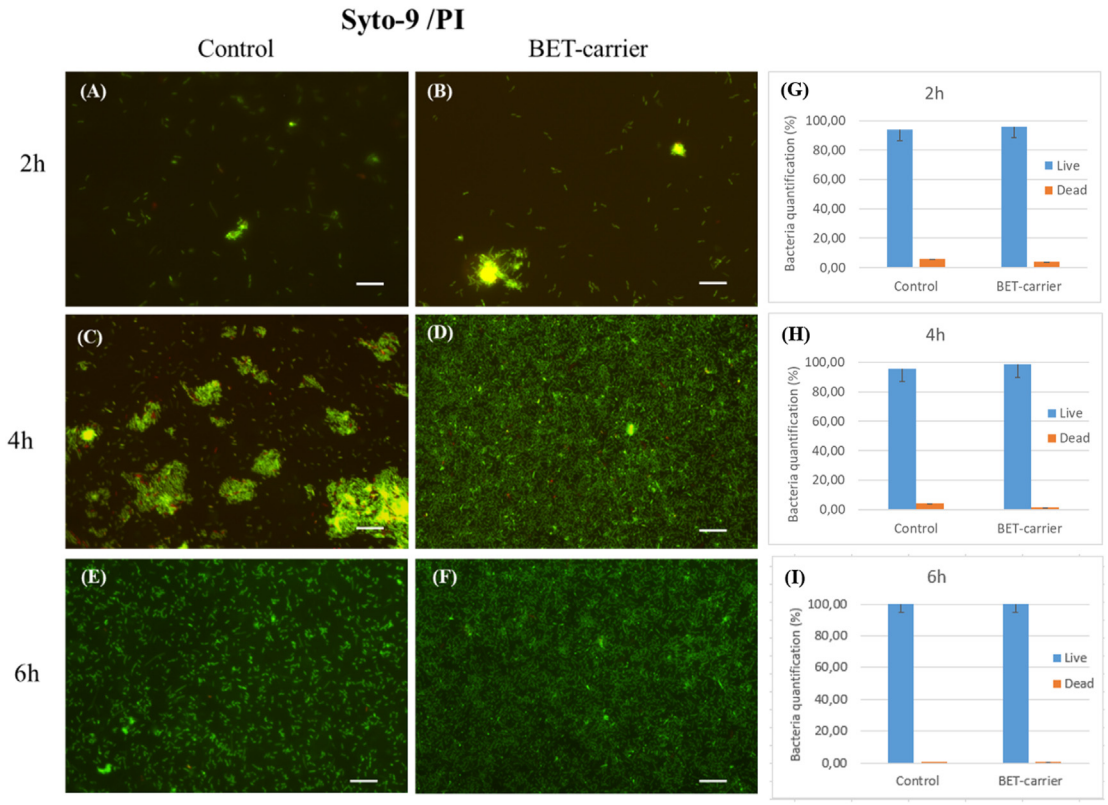

Fig. 8. Typical fluorescence microscopy images and live/dead staining of *E. coli* bacteria on the control (A, B, C) and BET-carrier (D, E, F) at the three incubation times. Scale bars indicate 20 μm. (G, H, I) Bacteria quantification in percentage of live *E. coli* cells (blue column) and dead (orange column) on the control and the BET-carrier, respectively, after 2 h, 4 h and 6 h of incubation. These data were obtained over three replicates of the experiments and over ten pictures recorded on the sheet surface for each replicate.

[47] (Image J 1.52a, http://imagej.nih.gov/ij, Java1.8.0_112, 64 bit), an open-source image-processing program developed at the National Institutes of Health (NIH, USA), to evaluate the mean values of the signal intensities for the green (SYTO 9) and the red (propidium iodide) channels, and hence to obtain information about the average amount of live and dead bacteria. The corresponding results are reported in Fig. 8 (G-I) where the columns refer to the percentage of live (blue columns) and dead (orange columns) bacteria. These results clearly show that the

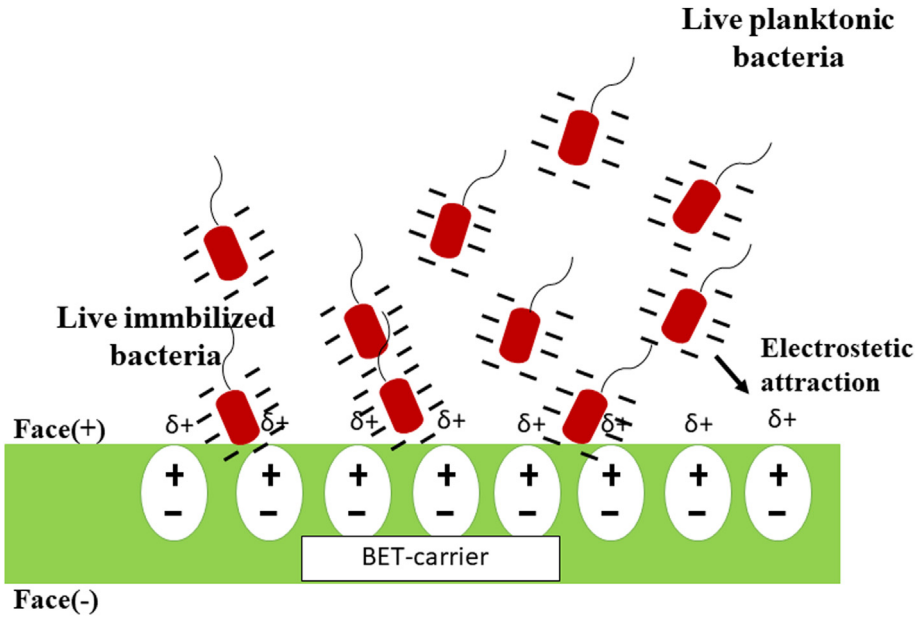

Fig. 9. Schematic view of the typical interaction of the bacterial cells with the BET-carrier. Face (+) and Face (−) indicate the polarity of the BET-carrier faces. In particular, the dipole orientation exhibits one surface with positive polarity (δ+), indicated by Face (+) in the scheme. The external surface of the bacteria cytoplasmic membrane exhibits a negative charge (−).

number of dead cells (orange columns) was negligible for both the control and the BET-carrier, thus demonstrating the biocompatibility of the sheets. In addition, the results show that the high-density biomass generated on the BET-carrier was viable for all of the three incubation stages studied in this work (2 h, 4 h, 6 h).

It is important to note that the distribution of the bacteria shown by the images of Figs. 6 and 8 are not comparable each other because they refer to two different sheets which were both "pyro-electrified" but then treated differently, one with CV staining and the other with the live/dead viability test. In other words, we cannot expect the same distribution of bacteria on the surface of each PE sheet. Conversely, the significant results are represented by the statistical data reporting the amount of bacteria on the surfaces (see graphs in Figs. 7 and 8 (G-I)).

Fig. 9 shows the schematic view of the typical interaction between the BET-carrier and the planktonic bacteria. The bacteria exhibit a net negative charge on the external surface of the cytoplasmic membrane. This is attracted electrostatically by the positive surface charge of the BET-carrier. This demonstrates definitely its ability to immobilize planktonic bacteria and to promote a biofilm formation more rapidly than the control, avoiding binding reactions that could damage the bacterial cytomembrane.

4. Conclusion

We performed here a quantitative determination of the biomass adhering on the BET-carrier in the very early stages of biofilm formation. We used the CV assay at different incubation times and for two bacterial concentrations, which OD differed by one order of magnitude. The results show that the biofilm on the BET-carrier is similar in nature to that formed on the control sheet.

Conversely, the significant difference regards the time of formation that is more rapid in case of the BET-carrier, even in case of highly diluted bacterial suspensions. This allowed us to evaluate rapidly the ability of the bacterial strain to form biofilm, avoiding the 24–48 h incubation times usually encountered in standard microbiology assays. Furthermore, since the interaction of different types of bacteria with the BET-carrier depends on an electrostatic interaction, and therefore on the degree of polarization of the bacterium itself, the technique can be used for the simultaneous culture of more bacterial strains. In such a way, the BET-carrier would allow the microbiologist to evaluate the prevalence of one of the species in the biofilm formation. In conclusion, we believe that the BET-carrier would be a promising candidate for testing very rapidly the ability of bacterial strains to form biofilm, even in case of low abundant samples. This would have a great impact for early detection of bacteria and for a rapid determination of antimicrobial susceptibility.

Author contributions

E.O. planned, conducted the experiments and wrote the manuscript. M.M. conducted the viability tests. F.N. prepared the biological cultures and supervised the experimental procedures. R.R. prepared the pyro-electrified sheets. P.F. and S.G. supervised the project. All authors contributed to the discussion of the results and to the preparation of the manuscript.

Declaration of competing interest

The authors declare that they have no known competing financial interests or personal relationships that could have appeared to influence the work reported in this paper.

Acknowledgment

The authors acknowledge the EU funding within the Horizon 2020 Program, under the FET-OPEN Project "SensApp", Grant Agreement n.829104. They also thank the Italian Ministry of Education University and Research for the financial support of an innovative research doctor for industrial characterization within the XXXIII cycle doctorate of the University Vanvitelli (DOT1649008).

Appendix A. Supplementary data

Supplementary data to this article can be found online at https://doi.org/10.1016/j.bioflm.2020.100040.

References

[1] Elizaquível P, Sánchez G, Aznar R. Quantitative detection of viable foodborne E. coli O157: H7, Listeria monocytogenes and Salmonella in fresh-cut vegetables combining propidium monoazide and real-time PCR. Food Contr. 2012;25(2):704–8. https://doi.org/10.1016/j.foodcont.2011.12.003.

[2] Devasia RA, Jones TF, Ward J, Stafford L, Hardin H, Bopp C, et al. Endemically acquired foodborne outbreak of enterotoxin-producing Escherichia coli serotype O169: H41. Am. J. Med. 2006;119(2):168-e7. https://doi.org/10.1016/j.amjmed.2005.07.063.

[3] Garrett TR, Bhakoo M, Zhang Z. Bacterial adhesion and biofilms on surfaces. Prog. Nat. Sci. 2008;18(9):1049–56. https://doi.org/10.1016/j.pnsc.2008.04.001.

[4] Bianco V, Mandracchia B, Nazzaro F, Rega R, Ferraro P, Grilli S. Detection of self-propelling bacteria by speckle correlation assessment and applications to food industry. In: Optical Methods for Inspection, Characterization, and Imaging of ACS Appl. Mater. Interfaces 2020 IV. International Society for Optics and Photonics, vol. 11060; 2019, 1106007. https://doi.org/10.1117/12.2527416.

[5] Truong VK, Lapovok R, Estrin YS, Rundell S, Wang JY, Fluke CJ, et al. The influence of nano-scale surface roughness on bacterial adhesion to ultrafine-grained titanium. Biomaterials 2010;31(13):3674–83. https://doi.org/10.1016/j.biomaterials.2010.01.071.

[6] Encinas N, Yang CY, Geyer F, Kaltbeitzel A, Baumli P, Reinholz J, et al. Submicrometer-sized roughness suppresses bacteria adhesion. ACS Appl. Mater. Interfaces 2020;12(19):21192–200. https://doi.org/10.1021/acsami.9b22621.

[7] González-Rivas F, Ripolles-Avila C, Fontecha-Umaña F, Ríos-Castillo AG, Rodríguez-Jerez JJ. Biofilms in the spotlight: detection, quantification, and removal methods. Compr. Rev. Food Sci. Food Saf. 2018;17(5):1261–76. https://doi.org/10.1111/1541-4337.12378.

[8] Hori K, Matsumoto S. Bacterial adhesion: from mechanism to control. Biochem. Eng. J. 2010;48(3):424–34. https://doi.org/10.1016/j.bej.2009.11.014.

[9] Teughels W, Van Assche N, Sliepen I, Quirynen M. Effect of material characteristics and/or surface topography on biofilm development. Clin. Oral Implants Res. 2006;17(S2):68–81. https://doi.org/10.1111/j.1600-0501.2006.01353.x.

[10] Terada A, Yuasa A, Kushimoto T, Tsuneda S, Katakai A, Tamada M. Bacterial adhesion to and viability on positively charged polymer surfaces. Microbiology 2006;152(12):3575–83. https://doi.org/10.1016/j.bej.2009.11.014.

[11] Mandracchia B, Palpacuer J, Nazzaro F, Bianco V, Rega R, Ferraro P, Grilli S. Biospeckle decorrelation quantifies the performance of alginate-encapsulated probiotic bacteria. IEEE J. Quant. Electron. 2018;25(1):1–6. https://doi.org/10.1109/JSTQE.2018.2836941.

[12] Linke D, Goldman A. Bacterial Adhesion: Chemistry, Biology and Physics. Springer Science & Business Media; 2011. p. 715.

[13] Mandracchia B, Nazzaro F, Bianco V, Rega R, Ferraro P, Grilli S. Assessment of bacteria microencapsulation performance through bio-speckle dynamic analysis. LBIS. Int. Soc. Opt. Photon. 2019;10890:108900L. https://doi.org/10.1117/12.2509440.

[14] Poortinga AT, Bos R, Norde W, Busscher HJ. Electric double layer interactions in bacterial adhesion to surfaces. Surf. Sci. Rep. 2002;47(1):1–32. https://doi.org/10.1016/S0167-5729(02)00032-8.

[15] Hermansson M. The DLVO theory in microbial adhesion. Colloids Surf. B Biointerfaces 1999;14(1–4):105–19. https://doi.org/10.1016/S0927-7765(99)00029-6.

[16] Azeredo J, Visser J, Oliveira R. Exopolymers in bacterial adhesion: interpretation in terms of DLVO and XDLVO theories. Colloids Surf. B Biointerfaces 1999;14(1–4):141–8. https://doi.org/10.1016/S0927-7765(99)00031-4.

[17] Emerson RJ, Camesano TA. Nanoscale investigation of pathogenic microbial adhesion to a biomaterial. Appl. Environ. Microbiol. 2004;70(10):6012–22. https://doi.org/10.1128/AEM.70.10.6012-6022.2004.

[18] Hayashi H, Tsuneda S, Hirata A, Sasaki H. Soft particle analysis of bacterial cells and its interpretation of cell adhesion behaviors in terms of DLVO theory. Colloids Surf. B Biointerfaces 2001;22(2):149–57. https://doi.org/10.1016/S0927-7765(01)00161-8.

[19] van Loosdrecht MC, Lyklema J, Norde W, Zehnder AJ. Bacterial adhesion: a physicochemical approach. Microb. Ecol. 1989;17(1):1–15.

[20] Azeredo J, Azevedo NF, Briandet R, Cerca N, Coenye T, Costa AR, et al. Critical review on biofilm methods. Crit. Rev. Microbiol. 2017;43(3):313–51. https://doi.org/10.1080/1040841X.2016.1208146.

[21] Olivares E, Badel-Berchoux S, Provot C, Jaulhac B, Prévost G, Bernardi T, Jehl F. The BioFilm Ring Test: a rapid method for routine analysis of Pseudomonas aeruginosa biofilm formation kinetics. J. Clin. Microbiol. 2016;54(3):657–61. https://doi.org/10.1128/JCM.02938-15.

[22] Gottenbos B, Van Der Mei HC, Busscher HJ, Grijpma DW, Feijen J. Initial adhesion and surface growth of Pseudomonas aeruginosa on negatively and positively

charged poly (methacrylates). J. Mater. Sci. Mater. Med. 1999;10(12):853–5. https://doi.org/10.1023/A:1008989416939.
[23] Harkes G, Dankert J, Feijen J. Growth of uropathogenic Escherichia coli strains at solid surfaces. J. Biomater. Sci. Polym. Ed. 1992;3(5):403–18. https://doi.org/10.1163/156856292X00213.
[24] Gennari O, Marchesano V, Rega R, Mecozzi L, Nazzaro F, Fratianni F, Ferraro P. Pyroelectric effect enables simple and rapid evaluation of biofilm formation. ACS Appl. Mater. Interfaces 2018;10(18):15467–76. https://doi.org/10.1021/acsami.8b02815.
[25] Rega R, Gennari O, Mecozzi L, Grilli S, Pagliarulo V, Ferraro P. Pyro-electrification of polymer membranes for cell patterning. In AIP Conf. Proc. 2016;1736(1):020042. https://doi.org/10.1063/1.4949617.
[26] Rega R, Gennari O, Mecozzi L, Grilli S, Pagliarulo V, Ferraro P. Bipolar patterning of polymer membranes by pyroelectrification. Adv. Mater. 2016;28(3):454–9. https://doi.org/10.1002/adma.201503711.
[27] Lettieri S, Rega R, Pallotti DK, Gennari O, Mecozzi L, Maddalena P, et al. Direct evidence of polar ordering and investigation on cytophilic properties of pyroelectrified polymer films by optical second harmonic generation analysis. Macromolecules 2017;50(19):7666–71. https://doi.org/10.1021/acs.macromol.7b00794.
[28] Rega R, Gennari O, Mecozzi L, Pagliarulo V, Mugnano M, Oleandro E, et al. Pyro-electrification of freestanding polymer sheets: a new tool for cation-free manipulation of cell adhesion in vitro. Front. Chem. 2019;7. https://doi.org/10.3389/fchem.2019.00429.
[29] Peitzsch M, Kiesel B, Harms H, Maskow T. Real time analysis of Escherichia coli biofilms using calorimetry. Chem. Eng. Process: Process Intensification 2008;47(6):1000–6. https://doi.org/10.1016/j.cep.2007.02.029.
[30] The Centers for Disease Control and Prevention (CDC). General information, Escherichia coli (E. coli). http://www.cdc.gov/ecoli/general/index.html. [Accessed 3 August 2012].
[31] Bhowmick S, Iodice M, Gioffrè M, Breglio G, Irace A, Riccio M, et al. Investigation of pyroelectric fields generated by lithium niobate crystals through integrated microheaters. Sensor Actuator Phys. 2017;261:140–50. https://doi.org/10.1016/j.sna.2017.05.010.
[32] Pagliarulo V, Gennari O, Rega R, Mecozzi L, Grilli S, Ferraro P. Twice electric field poling for engineering multiperiodic Hex-PPLN microstructures. Optic Laser. Eng. 2018;104:48–52. https://doi.org/10.1016/j.optlaseng.2017.08.015.
[33] Rega R, Gennari O, Mecozzi L, Pagliarulo V, Bramanti A, Ferraro P, Grilli S. Maskless arrayed nanofiber mats by bipolar pyroelectrospinning. ACS Appl. Mater. Interfaces 2019;11(3):3382–7. https://doi.org/10.1021/acsami.8b12513.
[34] Gennari O, Rega R, Mugnano M, Oleandro E, Mecozzi L, Pagliarulo V, et al. A skin-over-liquid platform with compliant microbumps actuated by pyro-EHD pressure. NPG Asia Mater. 2019;11(1):1–8. https://doi.org/10.1038/s41427-018-0100-z.
[35] https://www.dsmz.de/collection/catalogue/details/culture/DSM-6897.
[36] Zwietering MH, Jongenburger I, Rombouts FM, Van't Riet KJAEM. Modeling of the bacterial growth curve. Appl. Environ. Microbiol. 1990;56(6):1875–81.
[37] Buchanan RL, Whiting RC, Damert WC. When is simple good enough: a comparison of the Gompertz, Baranyi, and three-phase linear models for fitting bacterial growth curves. Food Microbiol. 1997;14(4):313–26.
[38] Widdel F. Theory and measurement of bacterial growth. Di dalam Grundpraktikum Mikrobiologie 2007;4(11):1–11.
[39] Christensen GD, Simpson WA, Younger JJ, Baddour LM, Barrett FF, Melton DM, et al. Adherence of coagulase-negative staphylococci to plastic tissue culture plates: a quantitative model for the adherence of staphylococci to medical devices. J. Clin. Microbiol. 1985;22(6):996–1006.
[40] Heo J, Thomas KJ, Seong GH, Crooks RM. A microfluidic bioreactor based on hydrogel-entrapped E. coli: cell viability, lysis, and intracellular enzyme reactions. Anal. Chem. 2003;75(1):22–6. https://doi.org/10.1021/ac0259717.
[41] Stepanović S, Vuković D, Dakić I, Savić B, Švabić-Vlahović M. A modified microtiter-plate test for quantification of staphylococcal biofilm formation. J. Microbiol. Methods 2000;40(2):175–9. https://doi.org/10.1016/S0167-7012(00)00122-6.
[42] Wakimoto N, Nishi J, Sheikh J, Nataro JP, Sarantuya JAV, Iwashita M, et al. Quantitative biofilm assay using a microtiter plate to screen for enteroaggregative Escherichia coli. Am. J. Trop. Med. Hyg. 2004;71(5):687–90. https://doi.org/10.4269/ajtmh.2004.71.687.
[43] Gjermansen M, Ragas P, Sternberg C, Molin S, Tolker-Nielsen T. Characterization of starvation-induced dispersion in Pseudomonas putida biofilms. Environ. Microbiol. 2005;7(6):894–904. https://doi.org/10.1111/j.1462-2920.2005.00775.x.
[44] Pratt LA, Kolter R. Genetic analysis of Escherichia coli biofilm formation: roles of flagella, motility, chemotaxis and type I pili. Mol. Microbiol. 1998;30(2):285–93. https://doi.org/10.1046/j.1365-2958.1998.01061.x.
[45] Jorgensen JH, Turnidge JD. Susceptibility Test Methods: Dilution and Disk Diffusion Methods Manual of Clinical Microbiology. eleventh ed. Washington DC: ASM Press; 2015.
[46] Rzhepishevska O, Hakobyan S, Ruhal R, Gautrot J, Barbero D, Ramstedt M. The surface charge of anti-bacterial coatings alters motility and biofilm architecture. Biomater. Sci. 2013;1(6):589–602.
[47] Abràmoff MD, Magalhães PJ, Ram SJ. Image processing with ImageJ. Biophot. Int. 2004;11(7):36–42.